ACS OMEGA

Open Access

http://pubs.acs.org/journal/acsodf

Article

In Vitro Nonalcoholic Fatty Liver Disease Model Elucidating the Effect of Immune Environment on Disease Progression and Alleviation

Inhye Kim,[‖] Mi-lang Kyun,[‖] Hyewon Jung, Ji-In Kwon, Jeongha Kim, Ju-Kang Kim, Yu Bin Lee,* Young-In Kwon,* and Kyoung-Sik Moon*

Cite This: *ACS Omega* 2024, 9, 25094−25105

Read Online

ACCESS | Metrics & More | Article Recommendations | Supporting Information

ABSTRACT: Nonalcoholic fatty liver disease (NAFLD), which is a major cause of chronic liver disease, is characterized by fat accumulation in the liver. Existing models struggle to assess medication effects on liver function in the context of NAFLD's unique inflammatory environment. We address this by developing a 3D in vitro NAFLD model using HepG2 and THP-1 cells (mimicking liver and Kupffer cells) cocultured using transwell and hydrogel system. This mimics liver architecture and allows for manipulation of the immune environment. We demonstrate that the model recapitulates key NAFLD features: steatosis (induced by fatty acids), oxidative stress, inflammation, and impaired liver function embodying the interrelationship between NAFLD and the surrounding immune environment. This versatile model offers a valuable tool for preclinical NAFLD research by incorporating a disease-relevant immune environment.

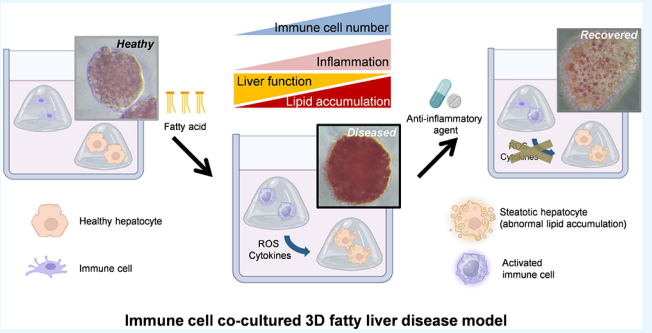

Immune cell co-cultured 3D fatty liver disease model

INTRODUCTION

The liver is the largest internal organ in the human body and performs various metabolic functions essential for maintaining life. These include regulating blood sugar, managing cholesterol, producing bile, and detoxifying harmful substances from both the body and external sources.[1] Among these functions, a crucial role of the liver is in lipid metabolism. The sequence of lipid metabolism can be briefly outlined as follows: (1) absorption of lipids and fatty acids, (2) synthesis of neutral fats and formation and storage of lipid droplets, and (3) lipid consumption.[2] Excessive fat intake affects lipid metabolism, resulting in an overabundance of lipid droplets. Accumulation of these droplets results in impaired liver function.[3] Fatty liver diseases include alcoholic fatty liver disease (ALD) and nonalcoholic fatty liver disease (NAFLD). ALD is primarily caused by chronic alcohol consumption.[4] In contrast, NAFLD is characterized by fat accumulation in the liver independent of alcohol intake and is linked to various risk factors, including high-fat diet, physical inactivity, obesity, type 2 diabetes, and genetic predisposition.[5] NAFLD is a growing global health concern due to the increasing prevalence of westernized dietary patterns.[6] NAFLD progresses through various pathological stages, including liver steatosis, nonalcoholic steatohepatitis (NASH), liver fibrosis, cirrhosis, and hepatocellular carcinoma (liver cancer).[7]

Continuous research and development are underway in the field of therapeutic interventions for NAFLD. Although pharmacological agents have demonstrated efficacy in diminishing hepatic lipid accumulation, adverse effects such as edema and cardiovascular complications may occur in some individuals.[8] Previous in vitro studies have addressed these concerns by directly exposing hepatocytes to oleic acid (OA) and palmitic acid (PA) in order to induce aberrant lipid accumulation. OA, a monounsaturated fatty acid, is naturally found in various animal and vegetable fats and oils.[9] On the other hand, PA, the most common saturated fatty acid found in animals, plants, and microorganisms, has also been utilized in numerous previous studies to induce steatosis in hepatocytes.[10] Subsequent treatment with candidate therapeutic substances confirmed the recovery and established a model for exploring potential compounds for NAFLD treatment.[11] However, the hepatic tissue consists of parenchymal and nonparenchymal cells, and immune responses, particularly inflammation, play a pivotal role in NAFLD progression.[12] The intra- and extrahepatic immune systems in the liver respond to exposure to risk factors, such as dietary fat and infections, by initiating

Received: March 12, 2024
Revised: May 14, 2024
Accepted: May 21, 2024
Published: May 27, 2024

an inflammatory response. This response involves the secretion of inflammatory cytokines such as IL-6 and TNF-α influencing the activity of lipolytic enzymes.[13] The liver tissue is then damaged by the inflammatory response, and exposure to reactive oxygen species (ROS) further accelerates fat accumulation.[14] Notably, existing research has been deficient in comprehensively considering and incorporating immune system simulations.[15] This poses constraints in verifying the efficacy of candidate drugs for steatosis and limits the detection of immune-related steatosis risks in pharmaceutical candidates, which may lead to immune-related side effects.[16]

Therefore, it is necessary to establish a preclinical liver model that reflects the human immune system in order to study NAFLD. To simulate liver tissue, HepG2 cells, a widely used commercial human hepatocyte cell line derived from liver cancer, have been extensively employed in related research. Kupffer cells are specialized mononuclear phagocytic cells that play an important role in shaping the immune environment in the liver. Therefore, a commercially available monocytic cell line THP-1 with HepG2 was cocultured. As demonstrated in previous studies, an increase in intrahepatic inflammation and progression of NAFLD correlate with an elevated population of Kupffer cells and recruited macrophages.[17] Accordingly, experiments were conducted to simulate population changes by adjusting the coculture ratio (10:1 or 10:5) of HepG2 cells and THP-1 monocytes. We hypothesized that an increased proportion of THP-1 cells would lead to an enhanced inflammatory environment, accelerating lipid accumulation. Conventional coculture models of hepatic and nonparenchymal cells have been established to facilitate direct cell−cell contact.[18] However, these approaches impose constraints on the specific analyses and considerations for each cell type used. The use of THP-1 as a suspension introduced limitations and concerns regarding cell invasion during coculture in transwells. Therefore, we used a gelatin-based hydrogel to encapsulate THP-1 cells in a suspended state. This encapsulation not only prevented direct cell−cell contact with HepG2 cells but also facilitated indirect coculture. In this environment, the two cell types interact via paracrine mechanisms. The model was designed (1) to simulate the environment of NAFLD through the coculture of immune cells with controlled immune cell ratios,[19] (2) examine differences in lipid accumulation based on fatty acid treatments and immune cell coculture, and (3) propose a model suitable for the alleviation of lipid formation through treatment with potential therapeutic substances, allowing for future validation of the effectiveness of candidate therapeutic agents.

MATERIALS AND METHODS

Materials. TRIzol reagent and collagenase type I powder were sourced from Thermo Fisher Scientific (Waltham, MA, USA), PCR primers were obtained from Bioneer (Daejeon, Korea), Cell Counting Kit-8 (CCK-8) from Dojindo (Kumamoto, Japan) Cellular Reactive Oxygen Species (ROS) assay kit from Abcam (ab113851) (Cambridge, UK), methacrylated gelatin (GelMA) powder from 3DMaterials (Anyang, Korea), bovine serum albumin (BSA) from GenDEPOT (Baker, TX, USA), and other materials including OA (O1383), PA (P5585), ORO solution (O1391), and prednisolone (P6004) were purchased from Sigma-Aldrich (St. Louis, MA, USA). The 24-well transwell inserts with a 0.4 μm pore size membrane were purchased from Corning (NY, USA). Microplate reader (SpectraMax iD3) and UV irradiation system (Omnicure S1500) were purchased from Molecular Devices (San Jose, CA, USA) and Excelita Technologies (Waltham, MA, USA), respectively.

Cell Culture. Cell cultures for all of the experiments were maintained at 37 °C under 5% CO_2 conditions. RPMI 1640 medium and penicillin−streptomycin (P/S) were procured from Thermo Fisher Scientific (Waltham, MA, USA), and fetal bovine serum (FBS) was obtained from HyClone (Logan, UT, USA). The human hepatocellular carcinoma cell line HepG2 and monocyte cell line THP-1 were purchased from the American Type Culture Collection (Manassas, VA, USA). The culture medium contained 10% heat-inactivated FBS supplemented with 1% P/S.

Formation of Immune Cell Cocultured NAFLD Model. HepG2 cells were cultured for 1 d to attach to a 24 well plate (1.0×10^5 cells/well) prior to the coculture. The THP-1 hydrogel was cultured in the upper well on the following day. The hydrogel for THP-1 encapsulation was formed via photo-cross-linking using ultraviolet (UV) light. GelMA powder was mixed at a concentration of 3.5 wt % in DMEM medium with 0.05% photoinitiator and dissolved at 37 °C in a water bath. THP-1 cells were harvested in sufficient quantities and centrifuged (200g for 3 min) to obtain cell pellets. The cell pellet was then mixed with an appropriate volume of the GelMA solution and evenly dispensed in 50 μL (1.0 or 5.0×10^4 of THP-1 were incorporated) onto a glass slide (Figure S1). After setting the UV lamp distance above the glass slide to 20 cm, GelMA photo-cross-linking was conducted by irradiation with UV light for 45 s (20 mW/cm^2), which resulted in the formation of a hydrogel with three-dimensionally encapsulated cells. The hydrogels were gently lifted with a spatula and cultured in 24-well Transwell inserts. The media were replaced with media containing or without OAPA, along with THP-1 culture, and cultured for 7 days. All the procedures were conducted in a biosafety cabinet.

For the 3D culture of HepG2 cells, the cells were aggregated into spheroids by culturing 2×10^6 cells in a spheroid culture dish for 1 day (2035080, LabSphero, LabToLab, Daejeon, Korea). The harvested spheroids were suspended at a density of 2×10^6 cells/mL in the aforementioned 3.5 wt % GelMA solution containing 0.05% photoinitiator. HepG2 spheroids (50 μL, 1.0×10^5 of HepG2 were incorporated) suspended in GelMA solution were cross-linked by irradiation with UV light at 20 mW/cm^2 for 45 s (Figure S1). Separately prepared hydrogels encapsulating HepG2 and THP-1 cells were placed in 24-well plates and cultured.

Preparation of Fatty Acid Treatment. PA powder was dissolved in 1 mL of 100% ethanol to achieve a concentration of 200 mM. This solution was further dissolved at 70 °C in a water bath. The dissolved PA solution was then diluted to a concentration of 2.5 mM in a 10% BSA (fatty acid-free) solution in RPMI, and then, the mixture was warmed for 10 min at 55 °C in a water bath. The solution was then cooled to room temperature.

OA was diluted to a concentration of 5 mM in a 10% BSA fatty acid-free solution in RPMI and treated for 30 min at 37 °C in a water bath. Both fatty acid solutions were then sterile-filtered using a 0.22 μm pore membrane filter, stored at 4 °C, and warmed to room temperature before use by dilution in culture media.

CCK-8 Assay. After HepG2 cells were plated in a 96-well culture plate, the culture medium was replaced with fresh medium containing OA and PA at a 2:1 molar ratio. The

https://doi.org/10.1021/acsomega.4c02433
ACS Omega 2024, 9, 25094−25105

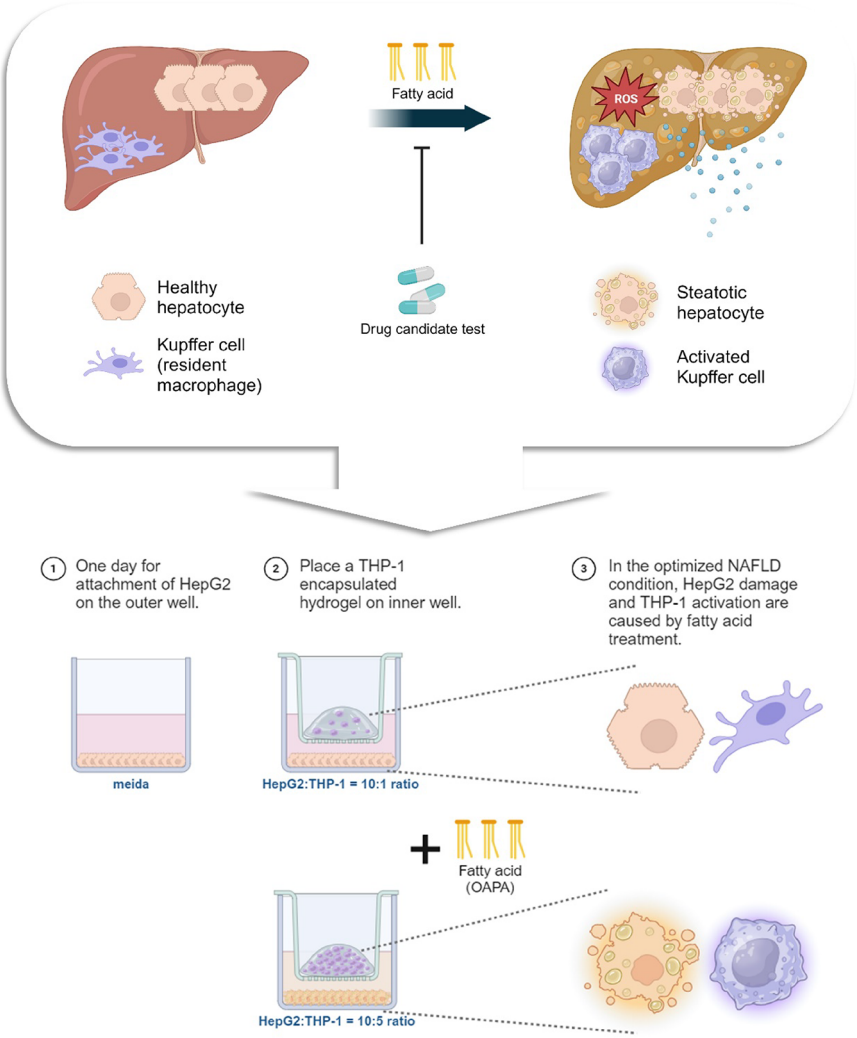

Figure 1. Schematic diagram of the NAFLD in vitro model considering both hepatocyte and immune environments (created with BioRender.com).

concentrations used were 320 and 160 μM; 160, 80 μM; 80, 40 μM; 40, 20 μM; 10, 5 μM; 5, 2.5 μM; and vehicle control. The medium was changed every 2 days, and the cells were cultured for 7 d (n = 4).

On day 7, the medium was removed, and fresh medium containing a 10:1 dilution of the CCK-8 reagent was added. The cells were then incubated for 1 h at 37 °C. Subsequently, the absorbance was measured at 490 nm to assess cell viability.

Oil Red O Staining. After completion of the culture period, the plate was washed with PBS. The cells were then fixed with a 4% paraformaldehyde solution at room temperature for 10 min. After fixation, the cells were washed twice with distilled water (DW) and treated with 60% isopropyl alcohol for 5 min, followed by removal to allow complete air-drying. Once the cells were dry, they were stained with 60% Oil Red O (ORO) solution at room temperature for 10 min (n = 6).

ImageJ software was used to measure the red signal intensities on the ORO stained images. The red color was extracted from the images, and the values of various regions with lipid droplets were measured. The mean and standard deviation were then calculated.

Cellular Reactive Oxygen Species Assay. THP-1 hydrogel and an equivalent amount of collagenase type I are mixed in a 1.5 mL tube and incubated at 37 °C for 30 min to dissolve the hydrogel. The experiments were conducted according to the manufacturer's protocol. The cells extracted from the hydrogel were washed with PBS, and an equivalent amount of DCFDA was added at a concentration of 20 nM. The cells are then incubated in the dark at 37 °C for 30 min (n = 6).

After washing with 1× buffer, the cells were resuspended and seeded at a density of 100,000 cells/well. Fluorescence is measured at Ex = 485 nm and Em = 535 nm.

Real-Time PCR. After washing with PBS, RNA was extracted using TRIzol reagent. RNA was quantified using a Nanodrop instrument, and cDNA synthesis was performed. Real-time PCR using the SYBR Green premix was conducted for 45 cycles using the QuantStudio5. Each cycle involved melting at 95 °C for 15 s, followed by annealing at 55 °C and extension at 75 °C. The CT values were used for data analysis. The relative expression levels of the target genes were normalized to those of the control group using β-actin. The experiment was conducted in triplicates (n = 3). Primers used in the experiments are listed in Supporting Information Table 1.

Statistical Analysis. The quantitative results presented in this paper are expressed as the mean ± standard deviation. Statistical significance was validated using Student's t-test and analysis of variance (ANOVA), with post hoc comparisons

https://doi.org/10.1021/acsomega.4c02433
ACS Omega 2024, 9, 25094−25105

conducted using Tukey's honest significant difference (HSD) test ($p < 0.05$).

RESULTS

Design of the InVitro NAFLD Model. The inflammation induced by abnormal lipid accumulation in the liver promotes NAFLD progression. By coculturing HepG2 and THP-1 cells, an artificial liver system mimicking the intrahepatic immune environment was established and treated with OAPA to induce in vitro steatosis (Figure 1). We implemented an indirect coculture system allowing interaction through paracrine effects without direct contact between THP-1 and HepG2 cells. This was mediated by gelatin-based hydrogel, inspired by collagen, which constitutes a significant portion of the extracellular matrix in the liver. We utilized gelatin derived from collagen as the raw material for the hydrogel. For photo-cross-linking using UV irradiation, methacrylated gelatin (GelMA) was introduced for encapsulation of THP-1 cells to maintain suspension state (Figure S1). The impact of the THP-1 coculture ratio on lipid accumulation was examined and assessed in order to determine whether treatment with agents that reduce inflammatory responses resulted in a decrease in lipid accumulation. THP-1 cells were collected separately from the hydrogel, and the relationship between immune cell behavior and lipid accumulation was investigated. HepG2 cells were also encapsulated in a 3D environment via the GelMA hydrogel to advance the model for better mimicking of physiological conditions. This model ultimately aimed to assess the effectiveness and safety of candidate drugs for NAFLD treatment, focusing on both hepatocytes and the immune system.

Lipid Accumulation of 2D Cultured HepG2 in a Response to the Treatment of OAPA. Prior to inducing the lipid formation in HepG2 cells, we investigated the effects of varying OAPA concentrations on HepG2 cell viability. The concentrations of OA and PA were varied as follows: (5:2.5), (10:5), (20:10), (40:20), (80:40), (160:80), and (320:160) μM. Cell viability was 96.0 ± 0.1% in the 5, 2.5 μM group, 90.0 ± 6.5% in the 10, 5 μM group, 93.0 ± 5.0% in the 20, 10 μM group, 78.0 ± 6.5% in the 40, 20 μM group, 67.0 ± 5.8% in the 80, 40 μM group, 55.0 ± 1.4% in the 160, 80 μM group, and 4.6 ± 6.6% in the 320, 160 μM group (Figure 2a). We induced lipid accumulation in HepG2 cells using two concentrations of OAPA: 10, 5 μM group ensuring cell viability was maintained above 75%, and a 40, 20 μM group which recorded viability below 70%. The red-stained lipid regions were barely detectable in the vehicle-treated control group. However, in the 10, 5 μM group, small red dots were partially visible, and in the 40, 20 μM group, prominently distributed and larger red-stained particles were observed, indicating an increased size with regard to the lipid-stained particles (Figure 2b).

Increased Lipid Accumulation by Hepatocyte Corresponding to THP-1 Coculture and Treatment of Fatty Acids. The OAPA concentrations were fixed at 10, 5 μM, for further experiments to minimize their effects on cell viability and functionalities. HepG2 and THP-1 cells were cocultured at cell ratios of 10:1 and 10:5. When subjected to the vehicle control (VC), neither coculture group showed notable lipid accumulation in HepG2 cells. Both coculture groups exhibited a notable increase in lipid accumulation following the ORO staining (Figure 3a). In addition, an increase in the number and size of lipid particles was evident in the 10:5 group compared to the 10:1 group (Figure 3a). Quantitative data on

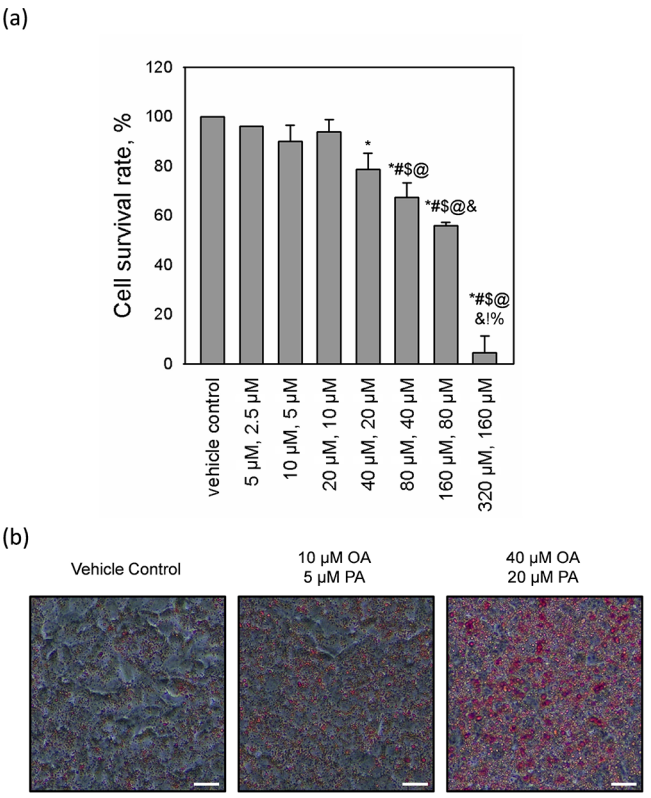

Figure 2. (a) Evaluation of the cellular viability across different concentrations of OA and PA. OA: PA of concentration: (5:2.5), (10:5), (20:10), (40:20), (80:40), (160:80), and (320:160) μM. "*", "#", "$", "@", "&", "!", and "%" indicate statistical significance in comparison with the vehicle control, (5:2.5), (10:5), (20:10), (40:20), (80:40), and (160:80) μM groups, respectively ($p < 0.05$). (b) ORO staining of HepG2 cells under various OAPA treatment conditions. Scale bars in the images are 20 μm (40× magnification).

lipid accumulation were obtained by measuring the red signal intensities of the ORO staining images (Figure 3b). The value for the 10:1 group treated with VC (HepG2 10:1_VC group) was normalized to 1.0 to calculate the relative lipid intensity in the other groups. In the 10:1 OAPA treatment group, the lipid intensity increased to 4.4 ± 0.9. In regard to the 10:5 conditions, the treatment of VC (HepG2 2:1_VC group) induced 3.8 ± 0.7, and the HepG2 2:1_OAPA group presented the highest lipid intensity of 6.1 ± 0.8. Collectively, lipid accumulation increased in response to the OAPA treatment as the ratio of THP-1 cells increased from 10:1 to 10:5. ROS are prominent indicators of cellular damage caused by inflammation and disease.[20] The production of ROS in THP-1 cells was quantified under various conditions (Figure 3c). The ROS detection value presented by THP-1 cells at a coculture ratio of 10:1 after VC treatment (THP-1 10:1_VC group) was used for normalization (1.0 ± 0.11). The THP-1 10:1_OAPA group showed a relative ROS production of 1.22 ± 0.12. Although the THP-1 10:5_VC group had five times more THP-1 cells compared to the THP-1 10:1_VC group, the group presented a relative ROS production of 3.27 ± 0.05. THP-1 10:5_OAPA cells showed the highest ROS production of 3.97 ± 0.16. However, this value was approximately 1.2 times higher than the relative ROS production in the THP-1 10:5_VC group, which is similar to the pattern observed in the THP-1 10:1 group. Despite an increase in the number of THP-1 cells, the changes in ROS production in response to the

https://doi.org/10.1021/acsomega.4c02433
ACS Omega 2024, 9, 25094−25105

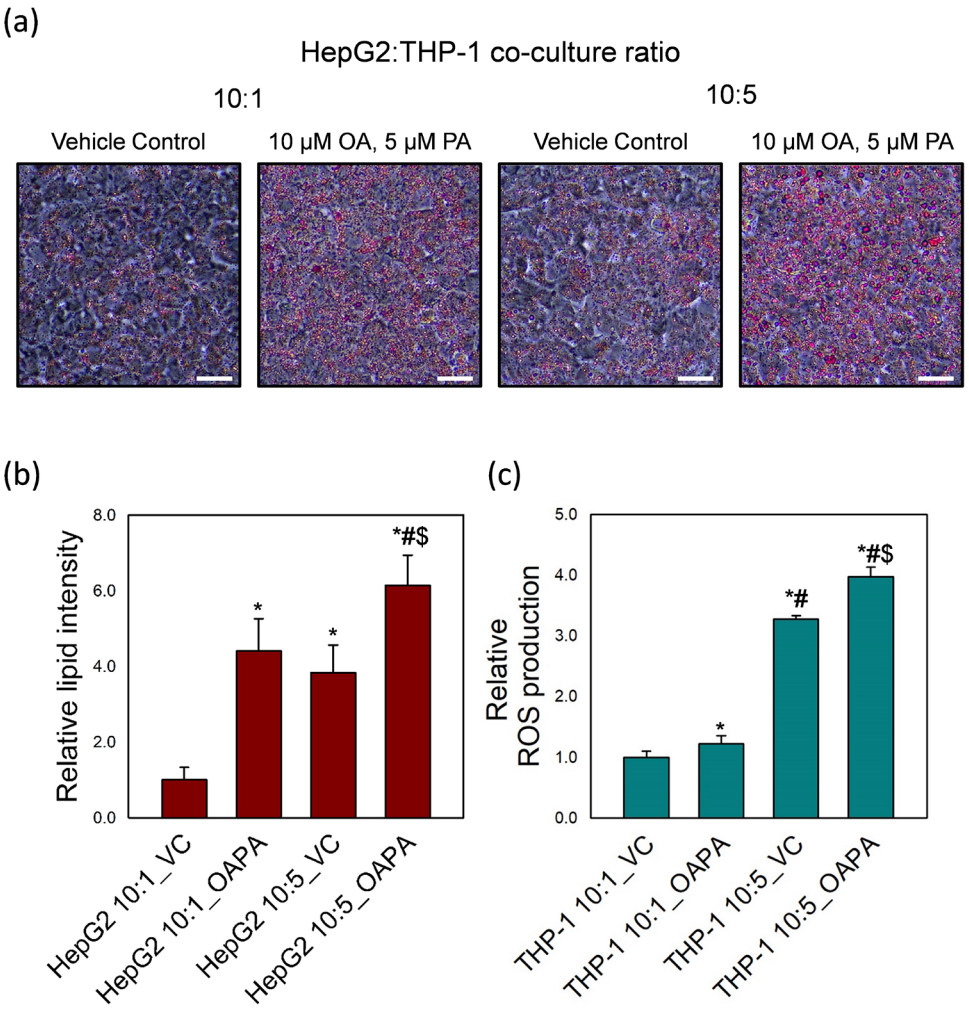

Figure 3. Evaluation of lipid accumulation by ORO staining in THP-1 cocultures and OAPA treatment. (a) ORO stained phase contrast images of HepG2 cells upon the varied culture conditions (scale bars = 20 μm, 40× magnification). (b) Relative lipid intensities under various culture conditions. "*", "#", and "$" indicate statistical significance compared to HepG2 10:1_VC, HepG2 10:1_OAPA, and HepG2 10:5_VC groups, respectively ($p < 0.05$). (c) Relative ROS production by THP-1 upon the varied experimental conditions. "*", "#", and "$" indicate statistical significance compared to THP-1 10:1_VC, THP-1 10:1_OAPA, and THP-1 10:5_OAPA groups, respectively ($p < 0.05$).

OAPA remained similar. However, increased ROS production with an increasing number of THP-1 cells indicated an association with an increase in the level of lipid accumulation.

Synergistic Increase in Inflammatory Responses and Decrease in Liver Functional Markers by the Cocultured THP-1 under Fatty Acid Treatment. The clinical symptoms of NAFLD include inflammation and accumulation of intracellular lipid droplets.[21] The gene expression levels related to inflammatory cytokines of IL-1β, IL-6, MCP-1, and TNF-α were examined after the harvest of HepG2 (Figure 4a). A significant increase in the expression of all four cytokines was observed when HepG2 and THP-1 cells were cocultured at a ratio of 10:5 and treated with OAPA (HepG2 10:5_OAPA group). The values presented on the HepG2 10:5_OAPA group are as follows: IL-1β, 1.39 ± 0.12; IL-6, 2.15 ± 0.24; MCP-1, 5.60 ± 1.23, and TNF-α, 3.32 ± 1.85. Changes in liver function markers (ALB, HNF4a, RBP4, and TTR) were assessed at the mRNA level under various culture conditions (Figure 4b). HepG2 10:1_VC and HepG2 10:1_OAPA groups did not exhibit remarkable changes upon the OAPA treatment. Notably, the HepG2 10:5_OAPA group exhibited the lowest expression level for all four key markers when compared to the other groups; ALB showed a significant reduction to 0.13 ± 0.01, HNF4α to 0.37 ± 0.23, RBP4 to 0.37 ± 0.10, and TTR to 0.10 ± 0.04. This indicates that an increase in the number of THP-1 cells creates a stronger inflammatory environment through the reaction with the lipid-containing OAPA, resulting in a significant decrease in liver functionality.

Reduction in ROS Production and Lipid Accumulation Derived from Suppressing Inflammatory Response through Prednisolone Treatment. In this experimental setup mimicking the immune environment of NAFLD, the alleviation of inflammation was examined through treatment with the well-known immunosuppressant prednisolone at 25 μM. The ORO staining images presented in Figure 6a reveal noticeably reduced lipid droplets in the HepG2 10:5_OAPA+Pred 25 μM group compared to the HepG2 10:5_OAPA group when prednisolone was cotreated with OAPA. In the result of relative lipid intensity, the group treated with prednisolone (HepG2 10:5_OAPA+Pred 25 μM) showed a significant decrease value of 1.07 ± 0.06 compared to HepG2 10:5_OAPA group showing 1.27 ± 0.13 (Figure 6b). The reduction in lipid intensity by prednisolone suggested a

https://doi.org/10.1021/acsomega.4c02433
ACS Omega 2024, 9, 25094−25105

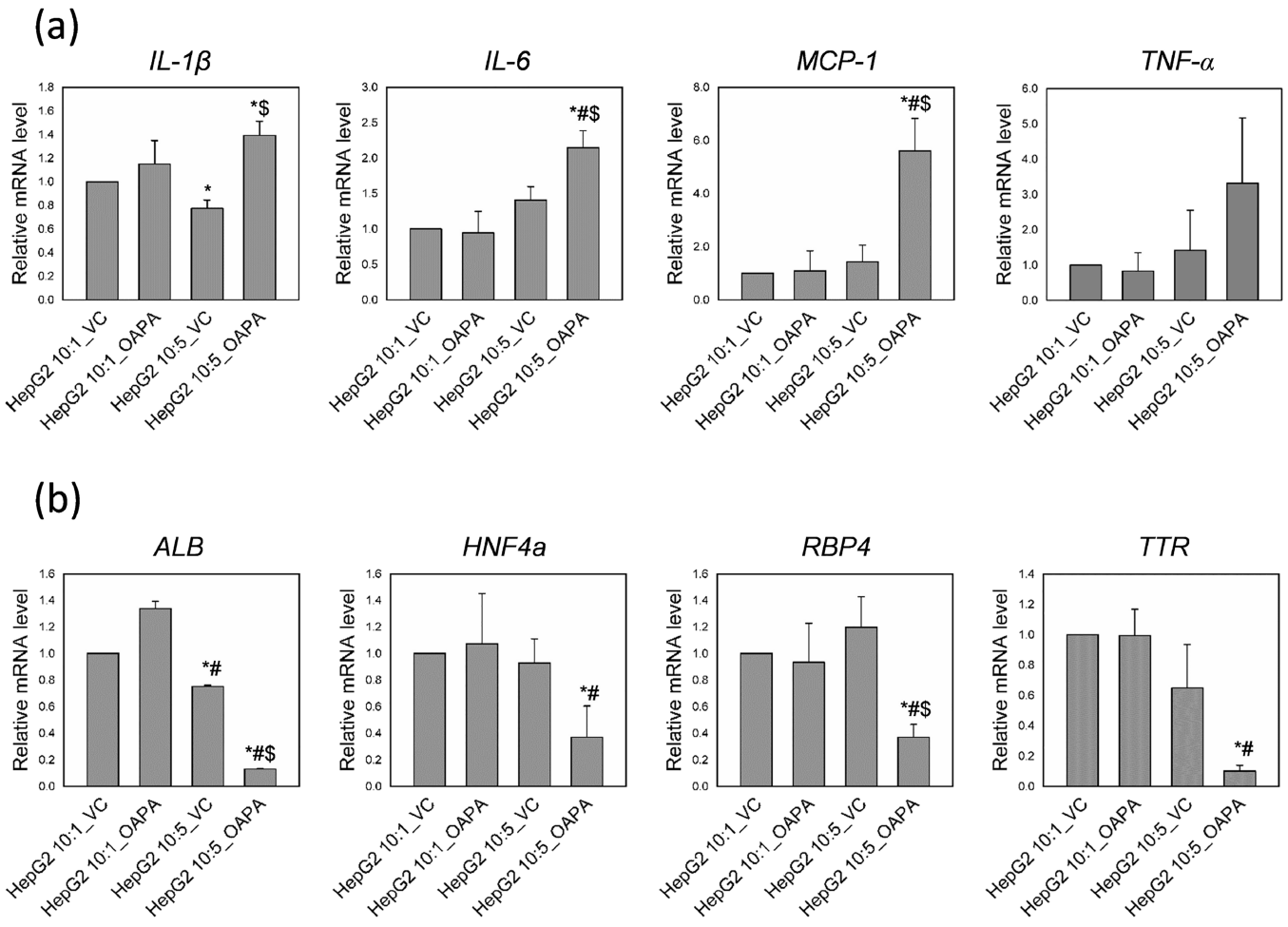

Figure 4. Expression levels of (a) inflammatory genes and (b) hepatic maturation markers in HepG2 cells after NAFLD induction. "*", "#", and "$" indicate statistical significance when compared to HepG2 10:1_VC, HepG2 10:1_OAPA, and HepG2 10:5_VC groups, respectively ($p < 0.05$).

recovery comparable to that of the control group (HepG2 10:5_VC), with no statistically significant difference. Furthermore, ROS production in THP-1 cells decreased following prednisolone treatment, suggesting a recovery level comparable to that in the control group (Figure 6c). These results suggest that suppressing inflammation in the immune microenvironment around liver cells could impede the progression of NAFLD.

Cross Validation of the Developed NAFLD Model using Three-Dimensional (3D) Culture System. Previous studies have demonstrated that three-dimensional (3D) culture techniques, such as spheroid formation and hydrogel encapsulation, provide a more physiologically relevant environment than using 2D cultures. This enhanced environmental similarity strengthens the functionality of hepatocyte cell lines.[22] In this study, we assembled HepG2 cells into three-dimensional (3D) spheroids encapsulated within the GelMA hydrogel to further mimic the hepatocyte environment in the human liver. The spheroids were encapsulated in a hydrogel to facilitate indirect coculture with THP-1 cells and allow cell-extracellular matrix (ECM) interactions. During the 7 days of culture, HepG2 spheroids within the hydrogel showed that spheroids composed of cells migrated into the hydrogel matrix (Figure 6a). The gene expression levels of the four hepatocyte maturation markers (ALB, HNFa, RBP4, and TTR) were also found to be significantly enhanced in regard to the 3D culture conditions when compared to those of the 2D condition (Figure 6b). We set the OA and PA concentration as 160 and 80 uM to induce the NAFLD conditions in the 3D construct, respectively. Although this concentration is relatively low compared to the values observed in NAFLD patients (>1000 uM),[23] it implies that cells cultured in 3D may have a greater capacity to withstand risk factors closer to those encountered in clinical settings as compared to 2D culture platform.[24] ORO staining was conducted on 3D cultured HepG2 constructs with various THP-1 coculture ratios (10:1 and 10:5). The objective was to investigate whether a comparable trend in lipid accumulation could be exhibited under 3D conditions, similar to the observations using the 2D culture platform (Figure 6(c)). The 3D HepG2 spheroids under a 10:1 coculture ratio with THP-1 cells exhibited a slight increase in lipid droplets following the OAPA treatment, whereas under the 10:5 coculture ratio conditions, more pronounced lipid accumulation appeared throughout the spheroids with a distinctive red signal. The results of image analysis for relative lipid intensity were normalized to the value of the vehicle control-treated group with a 10:1 coculture ratio (3D HepG2 10:1_VC) (Figure 6d). In the presence of OAPA, the group with the 10:1 ratio increased the lipid intensity to 2.44 ± 1.35. In groups with a 10:5 coculture ratio, the VC treated group showed a value of 2.95 ± 0.89, and a significant increase in lipid intensity to 5.42 ± 0.53 was observed after the OAPA treatment (3D

https://doi.org/10.1021/acsomega.4c02433
ACS Omega 2024, 9, 25094−25105

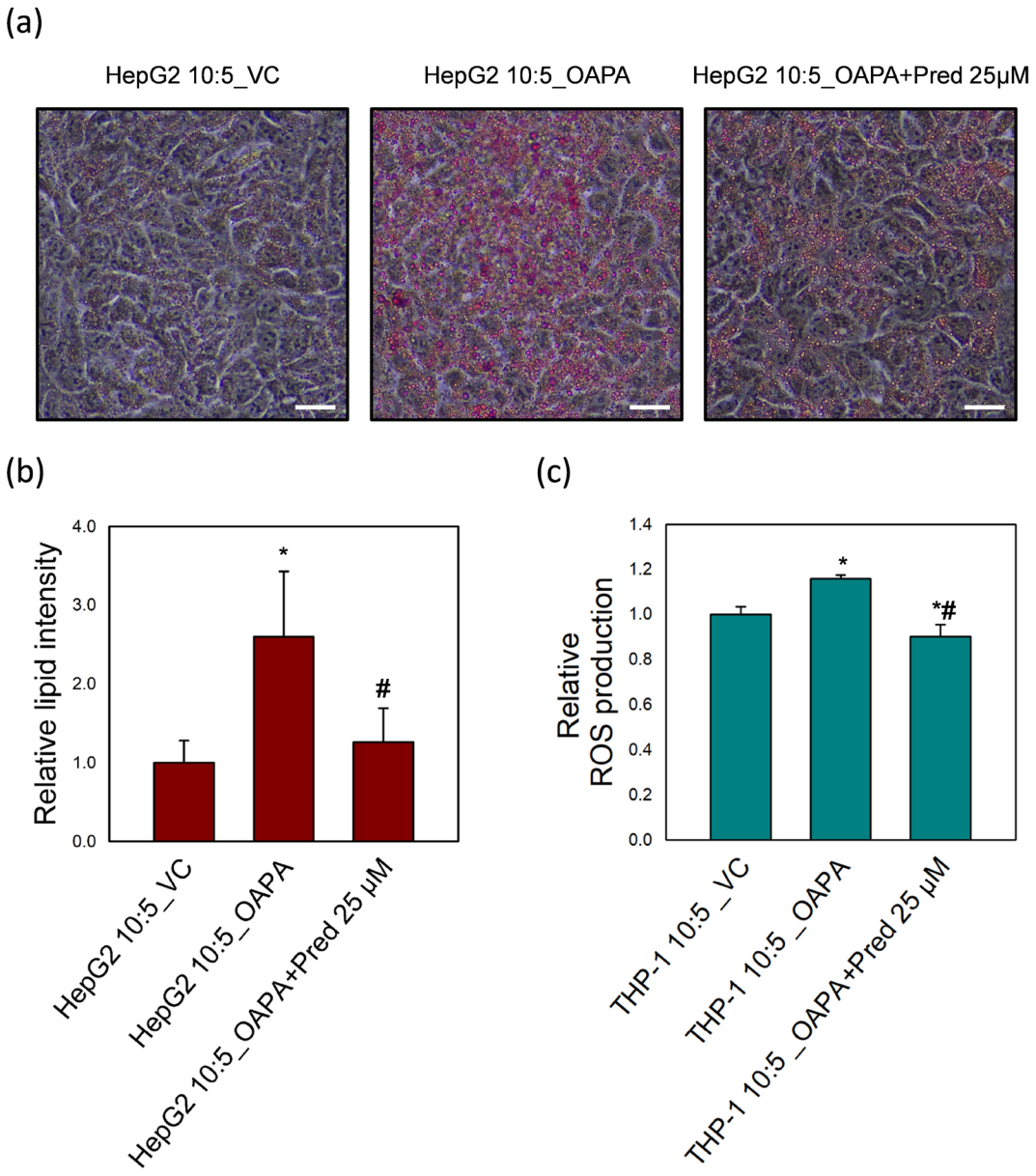

Figure 5. Alleviation of induced NAFLD using prednisolone. (a) ORO staining images of HepG2 after NALFD induction and alleviation (scale bars = 20 μm). (b) Relative lipid intensity after NALFD induction and alleviation. "*" and "#" indicate statistical significance compared to the HepG2 10:5_VC and HepG2 10:5_OAPA groups, respectively ($p < 0.05$). (c) Relative ROS production by THP-1 cells after NALFD induction and alleviation. "*" and "#" indicate statistical significance when compared to the THP-1 10:5_VC and THP-1 10:5_OAPA groups, respectively ($p < 0.05$).

HepG2 10:5_OAPA). These findings under 3D culture conditions indicated a notable elevation in the lipid intensity with an augmented THP-1 cell count, and OAPA treatment was aligned with the 2D culture conditions. We measured relative ROS production in order to investigate the association between lipid accumulation in 3D-cultured HepG2 cells and ROS generation in THP-1 cells (Figure 6e). The data revealed a noteworthy increase in the relative ROS production under NAFLD-like conditions (THP-1 10:5_OAPA). The highest relative ROS production was observed in the THP-1 10:5_OAPA group by measuring 3.18 ± 0.10. This underscores the necessity of incorporating the immune environment into an in vitro NAFLD model.

Similar to the inhibition of lipid accumulation observed under 2D culture conditions, we investigated the effect of prednisolone on lipid accumulation and ROS production in a 3D cultured model. As anticipated, prednisolone treatment in the NAFLD-induced group resulted in decreased lipid intensity to a level similar to that seen in the control group (Figure 7b). The increase in the relative ROS production following the OAPA treatment was markedly diminished by prednisolone treatment (Figure 7c). However, prednisolone is also known to exhibit hepatotoxicity.[25] In addition, long-term use of prednisolone can lead to glucocorticoid-induced osteopenia and sarcopenia, which are conditions shared by multiple diseases including NALFD.[26] Increased gene expression levels of hepatic damage markers of CRP, HAMP, and C3 genes were observed following treatment of the model with OAPA, and even higher increases in the damage marker expression were observed after prednisolone treatment (Figure S2). This

https://doi.org/10.1021/acsomega.4c02433
ACS Omega 2024, 9, 25094−25105

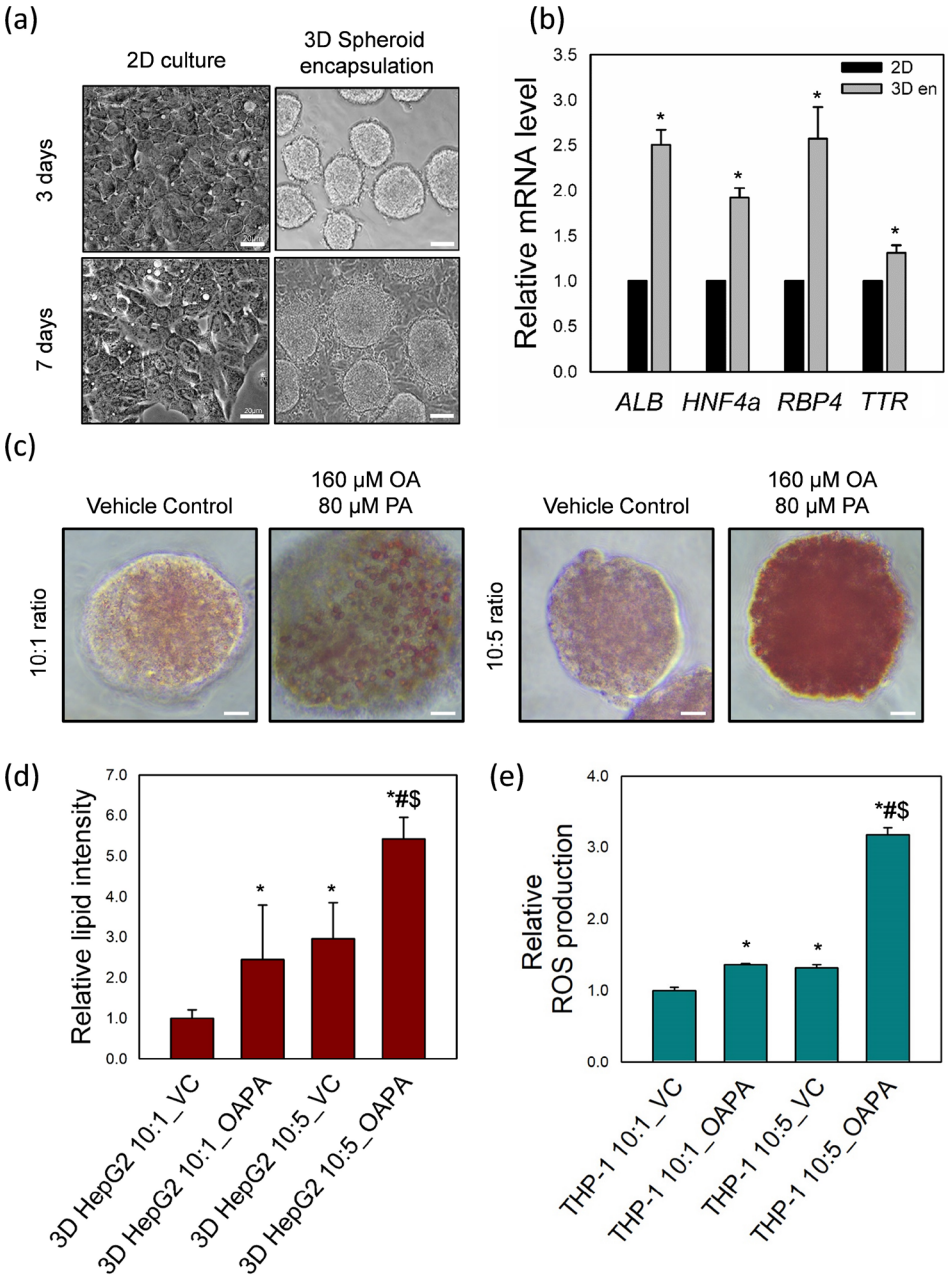

Figure 6. (a) Phase-contrast images of HepG2 cells cultured in D (left, scale bars = 20 μm) and encapsulated HepG2 spheroids within 3D GelMA hydrogels (right, scale bars = 50 μm). (b) Expression levels of genes associated with hepatocyte maturation in 2D and 3D cultures of HepG2 cells (*$p < 0.05$). (c) ORO-stained HepG2 spheroids in 3.5 wt % GelMA hydrogel under various NAFLD induction conditions (scale bars = 20 μm, 20× magnification). (d) Relative lipid intensity on the 3D HepG2 spheroids under various NAFLD induction conditions. "*", "#", and "$" indicate statistical significance compared to 3D HepG2 10:1_VC, 3D HepG2 10:1_OAPA, and 3D HepG2 10:5_VC groups, respectively ($p < 0.05$). (e) Relative ROS production by THP-1 upon the varied experimental conditions. "*", "#", and "$" indicate statistical significance compared to THP-1 10:1_VC, THP-1 10:1_OAPA, and THP-1 10:5_OAPA groups, respectively ($p < 0.05$).

pattern is similar to the existing reports on prednisolone-induced hepatotoxicity, despite the reduced lipid accumulation due to the alleviation of the inflammatory environment by prednisolone. This demonstrates the successful implementation of the 3D culture technique, providing a model for exploring avenues to overcome NAFLD from both the hepatocytic and immune perspectives.

■ DISCUSSION

In this study, a cell-based preclinical evaluation model was established to reflect the abnormal accumulation of intrahepatic lipids accompanied by inflammation seen in NAFLD. By coculturing HepG2 cells with THP-1 cells to mimic human liver tissue, changes in the lipid accumulation patterns of hepatocytes were observed in response to the immune environment. Before lipid generation was assessed, a concentration screening was conducted in order to determine whether OA or PA treatment induced cell death. In cell-based preclinical evaluations, conditions with cell survival rates exceeding 75% are generally considered nontoxic.[27] Based on the screening results using various concentrations, as shown in Figure 2a, two safe concentrations of (10, 5) and (40, 20) μM

https://doi.org/10.1021/acsomega.4c02433
ACS Omega 2024, 9, 25094−25105

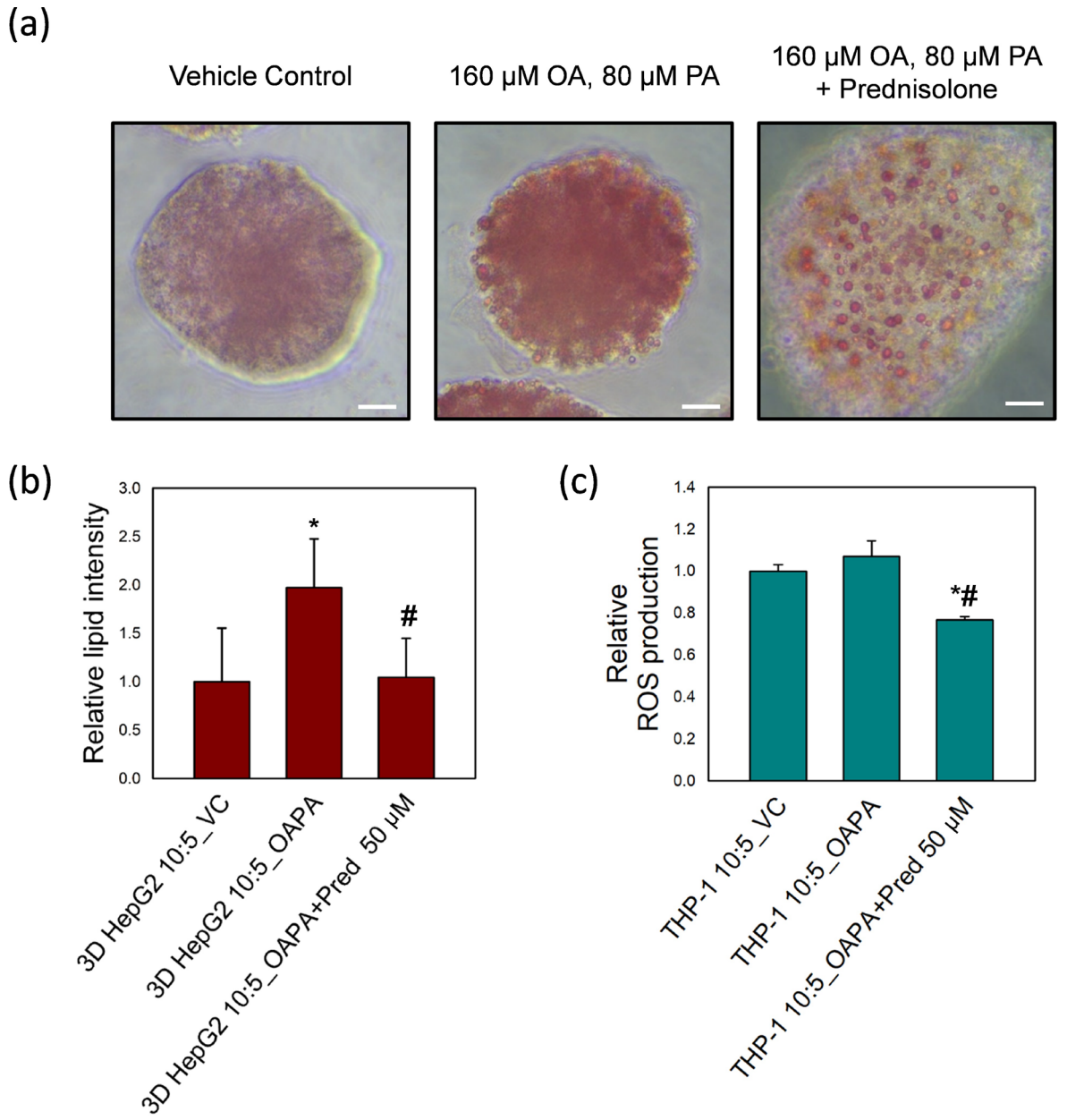

Figure 7. (a) ORO staining images of 3D cultured HepG2 cells after NALFD induction and alleviation by prednisolone treatment (scale bars = 20 μm). (b) Relative lipid intensity after NALFD induction and alleviation. "*" and "#" indicate statistical significance compared to the HepG2 10:5_VC and HepG2 10:5_OAPA groups, respectively ($p < 0.05$). (c) Relative ROS production by THP-1 cells after NALFD induction and alleviation. "*" and "#" indicate statistical significance when compared to the THP-1 10:5_VC and THP-1 10:5_OAPA groups, respectively ($p < 0.05$).

were chosen, where cell survival exceeded 75%. Subsequently, lipid accumulation was induced in HepG2 cells under selected conditions. The treatment results revealed a concentration-dependent facilitation of lipid accumulation, and no signs of cellular damage were observed during the 7 days of culture. The main hypothesis of this study was to enhance lipid accumulation through the application of a simulated immune system. Therefore, the baseline treatment conditions were chosen as the lower concentration of 10 μM OA and 5 μM PA.

The effect of THP-1 coculture and its ratio on lipid accumulation was determined to reflect the immune environment under fatty acid treatment and also to increase the severity of NAFLD. According to previous studies, the ratio of parenchymal cells to Kupffer cells under healthy conditions is approximately 10:1.[28] However, in NAFLD and other liver diseases, the ratio of Kupffer cells within the liver tissue increases to 10:4 due to the induction of inflammatory responses.[28] Our observations in this model are similar to those seen in previous reports that showed accelerated lipid formation accompanied by an inflammatory environment in response to fatty acids.[8,11] The inflammatory response, a significant characteristic of NAFLD,[29] was also evident at the gene level (Figure 5a). The expression levels of inflammatory cytokines known to be secreted during NAFLD, such as IL-1β, IL-6, MCP-1, and TNF-α,[30] were higher in the groups with the 10:5 coculture ratio with OAPA treatment. This differential gene expression suggests that an increased THP-1 cell ratio contributes to an inflammatory environment. Elevated levels of

https://doi.org/10.1021/acsomega.4c02433
ACS Omega 2024, 9, 25094−25105

ROS, key inflammatory markers, were seen using an established system. This substantiated the capability of the model to mimic the onset of NAFLD, effectively reflecting changes in the human immune system.[31] Furthermore, consistent with the clinical symptoms of hepatocyte damage in NASH characterized by concurrent lipid accumulation and inflammation, a significant reduction in the four hepatocyte function markers was observed when THP-1 cells were cultured at a ratio of 10:5 with OAPA treatment.[32]

Prednisolone is a steroid medication used to alleviate various clinical symptoms associated with inflammation. It is primarily used to treat conditions related to inflammation, allergic reactions, and immune system disorders.[25] Upon simultaneous treatment with OAPA and prednisolone for 7 days, a substantial decrease in lipid accumulation was observed in the model, indicating the potential to alleviate fatty-acid-induced pathological lipid deposition through anti-inflammatory treatment. However, the enhancement of hepatic damage marker expression levels by prednisolone demonstrates that prednisolone is an ideal drug for NAFLD treatment (Figure S2).

3D hepatocyte cultures offering additional advantages for human simulation have been implemented in previously developed models.[18] The increased gene expression levels of mature hepatic markers in 3D culture compared to 2D culture signify advanced emulation of human liver tissue and the development of more functional liver constructs.[22] Furthermore, noticeable differences in the extent of the ORO staining and ROS generation indicated the enhanced sensitivity of the 3D model to the induced NAFLD conditions. Therefore, a model aimed at more advanced simulations of human pathology was established by integrating 3D culture methods. This applies not only to HepG2 cells but also to other hepatocytes such as HepaRG and stem cell-derived hepatocytes; therefore, it can be improved into a more functional and physiologically relevant model. Furthermore, consideration should also be given to the source of immune cells, such as primary Kupffer cells. Especially with the emerging focus on personalized biotherapeutic development, the application of primary cells for constructing individualized preclinical evaluation models may be necessary. However, with the change in cell source, it would be essential to recognize that several conditions such as 3D encapsulation method and coculture ratios would need to be optimized.

Although ALD and NAFLD have different etiologies, they share many common features. Both conditions exhibit common mechanisms and events leading to hepatocellular fat accumulation, inflammation, and liver damage. Key downstream molecular events include fatty acid oxidation, inflammatory signaling, cell death, and increased levels of plasminogen activator inhibitor-1 (PAI-1).[33] This study has limitations as we did not investigate cell death and PAI. However, our model demonstrates the interrelation between the common mechanisms of inflammatory environment induction and lipid accumulation. Therefore, it is anticipated that it will contribute to the validation of therapeutic agents for fatty liver diseases, including not only NAFLD but also ALD.

Despite these achievements, this study has several limitations. In order to achieve a more precise analysis of immune environmental changes within the model, THP-1 cells were analyzed using flow cytometry, which is a widely employed method in immune cell analysis.[34] Functional analysis of hepatocytes was primarily conducted at the gene level using qRT-PCR. However, the addition of protein-level analyses, such as Western blotting and immunofluorescence staining, enhanced the overall completeness of the study. To reduce lipid formation in this model via nutraceuticals, it would be necessary to test commercially available therapeutic agents such as metformin and vitamin C.[23,35]

CONCLUSIONS

This study proposes an in vitro model that clearly illuminates the impact of simulated immune environments on the development and treatment of NAFLD by coculturing hepatocytes with immune cells. Lipid accumulation in HepG2 cells following fatty acid treatment was found to vary significantly based on the coculture conditions and different ratios of THP-1, emphasizing the significant influence of the immune microenvironment around the liver on the progression of NAFLD. In addition, treatment with anti-inflammatory agents alleviates abnormal lipid accumulation, further highlighting the importance of the immune environment in disease model development. With further improvements, this model can be applied to the development and validation of therapeutic candidates to overcome NAFLD.

ASSOCIATED CONTENT

Data Availability Statement

The data underlying this study are available in the published article and its Supporting Information.

Data Availability Statement

The datasets used and/or analyzed during the present study are available from the corresponding author on reasonable request.

Supporting Information

The Supporting Information is available free of charge at https://pubs.acs.org/doi/10.1021/acsomega.4c02433.

Additional table for PCR primer sequences, chemical structure of Gel-MA hydrogel for 3D cell culture, and expression levels of liver damage markers in the 3D model (PDF)

AUTHOR INFORMATION

Corresponding Authors

Yu Bin Lee − *Department of Advanced Toxicology Research, Korea Institute of Toxicology, Daejeon 34114, Republic of Korea;* orcid.org/0000-0002-1470-6499; Email: yubin.lee@kitox.re.kr

Young-In Kwon − *Department of Food and Nutrition, Hannam University, Daejeon 34430, Republic of Korea;* orcid.org/0000-0002-8069-8212; Email: youngk@hnu.kr

Kyoung-Sik Moon − *Department of Advanced Toxicology Research, Korea Institute of Toxicology, Daejeon 34114, Republic of Korea; Human and Environmental Toxicology, University of Science and Technology, Daejeon 34113, Republic of Korea*; Email: ksmoon@kitox.re.kr

Authors

Inhye Kim − *Department of Advanced Toxicology Research, Korea Institute of Toxicology, Daejeon 34114, Republic of Korea; Department of Food and Nutrition, Hannam University, Daejeon 34430, Republic of Korea*

https://doi.org/10.1021/acsomega.4c02433
ACS Omega 2024, 9, 25094−25105

Mi-lang Kyun − *Department of Advanced Toxicology Research, Korea Institute of Toxicology, Daejeon 34114, Republic of Korea*
Hyewon Jung − *Department of Advanced Toxicology Research, Korea Institute of Toxicology, Daejeon 34114, Republic of Korea; Human and Environmental Toxicology, University of Science and Technology, Daejeon 34113, Republic of Korea*
Ji-In Kwon − *Department of Advanced Toxicology Research, Korea Institute of Toxicology, Daejeon 34114, Republic of Korea; Department of Food and Nutrition, Hannam University, Daejeon 34430, Republic of Korea*
Jeongha Kim − *Department of Advanced Toxicology Research, Korea Institute of Toxicology, Daejeon 34114, Republic of Korea; Department of Food and Nutrition, Hannam University, Daejeon 34430, Republic of Korea*
Ju-Kang Kim − *Department of Advanced Toxicology Research, Korea Institute of Toxicology, Daejeon 34114, Republic of Korea*

Complete contact information is available at: https://pubs.acs.org/10.1021/acsomega.4c02433

Author Contributions

[‖]I.K. and M.-l.K. contributed equally to this study as the first authors.

Author Contributions

I.K. and M.-l.K. were responsible for data curation, writing the original draft, investigation, methodology, and formal analysis; H.J. and J.-I.K. were responsible for data curation, methodology, and formal analysis; J.K. and J.-K.K. were responsible for methodology and formal analysis; Y.B.L. was responsible for supervision, data curation, investigation, writing the review, and editing. Y.-I.K. was responsible for supervision, investigation, writing the review, and editing. K.S.M. was responsible for supervision, funding acquisition, and project administration. All the authors read and approved the manuscript.

Notes

The authors declare no competing financial interest.
There are no animal experiments carried out for this article.

■ ACKNOWLEDGMENTS

This study was supported by the Korea Institute of Toxicology, Republic of Korea (grant no. 1711195891).

■ REFERENCES

(1) Rui, L. Energy metabolism in the liver. *Comprehensive Physiology* **2014**, *4* (1), 177−197. From NLM
(2) de la Rosa Rodriguez, M. A.; Deng, L.; Gemmink, A.; van Weeghel, M.; Aoun, M. L.; Warnecke, C.; Singh, R.; Borst, J. W.; Kersten, S. Hypoxia-inducible lipid droplet-associated induces DGAT1 and promotes lipid storage in hepatocytes. *Molecular metabolism* **2021**, *47*, No. 101168. From NLM.
(3) Pei, K.; Gui, T.; Kan, D.; Feng, H.; Jin, Y.; Yang, Y.; Zhang, Q.; Du, Z.; Gai, Z.; Wu, J.; et al. An Overview of Lipid Metabolism and Nonalcoholic Fatty Liver Disease. *BioMed Res. Int.* **2020**, *2020*, No. 4020249. From NLM Torruellas, C.; French, S. W.; Medici, V. Diagnosis of alcoholic liver disease. *World journal of gastroenterology* **2014**, *20* (33), 11684−11699. From NLM
(4) Idalsoaga, F.; Kulkarni, A. V.; Mousa, O. Y.; Arrese, M.; Arab, J. P. Non-alcoholic Fatty Liver Disease and Alcohol-Related Liver Disease: Two Intertwined Entities. *Frontiers in medicine* **2020**, *7*, 448. From NLM
(5) Younossi, Z. M.; Golabi, P.; Paik, J. M.; Henry, A.; Van Dongen, C.; Henry, L. The global epidemiology of nonalcoholic fatty liver disease (NAFLD) and nonalcoholic steatohepatitis (NASH): a systematic review. *Hepatology (Baltimore, Md.)* **2023**, *77* (4), 1335−1347 DOI: 10.1097/hep.0000000000000004.. From NLM
(6) Machado, M. V.; Cortez-Pinto, H. Non-alcoholic fatty liver disease: what the clinician needs to know. *World journal of gastroenterology* **2014**, *20* (36), 12956−12980. From NLM
(7) Abd El-Kader, S. M.; El-Den Ashmawy, E. M. Non-alcoholic fatty liver disease: The diagnosis and management. *World J. Hepatol.* **2015**, *7* (6), 846−858. From NLM
(8) Francque, S.; Vonghia, L. Pharmacological Treatment for Non-alcoholic Fatty Liver Disease. *Advances in therapy* **2019**, *36* (5), 1052−1074. From NLM
(9) Choulis, N. H. Chapter 49 - Miscellaneous drugs, materials, medical devices, and techniques. *Side Eff. Drugs Annu.* **2009**, *31*, 757.
(10) Moravcová, A.; Červinková, Z.; Kučera, O.; Mezera, V.; Rychtrmoc, D.; Lotková, H. The effect of oleic and palmitic acid on induction of steatosis and cytotoxicity on rat hepatocytes in primary culture. *Physiological research* **2015**, *64* (Suppl5), S627−636. From NLM Murru, E.; Manca, C.; Carta, G.; Banni, S. Impact of Dietary Palmitic Acid on Lipid Metabolism. *Frontiers in Nutrition***2022**, *9*, 861664Mini Review. DOI: DOI: 10.3389/fnut.2022.861664.
(11) Schilcher, K.; Dayoub, R.; Kubitza, M.; Riepl, J.; Klein, K.; Buechler, C.; Melter, M.; Weiss, T. S. Saturated Fat-Mediated Upregulation of IL-32 and CCL20 in Hepatocytes Contributes to Higher Expression of These Fibrosis-Driving Molecules in MASLD. *Int. J. Mol. Sci.* **2023**, *24* (17), 13222.
(12) Ma, D. W.; Ha, J.; Yoon, K. S.; Kang, I.; Choi, T. G.; Kim, S. S. Innate Immune System in the Pathogenesis of Non-Alcoholic Fatty Liver Disease. *Nutrients* **2023**, *15* (9), 2068.
(13) Yang, A.; Mottillo, E. P. Adipocyte lipolysis: from molecular mechanisms of regulation to disease and therapeutics. *Biochemical journal* **2020**, *477* (5), 985−1008. From NLM
(14) Tang, S. P.; Mao, X. L.; Chen, Y. H.; Yan, L. L.; Ye, L. P.; Li, S. W. Reactive Oxygen Species Induce Fatty Liver and Ischemia-Reperfusion Injury by Promoting Inflammation and Cell Death. *Front Immunol* **2022**, *13*, No. 870239. From NLM
(15) Dallio, M.; Sangineto, M.; Romeo, M.; Villani, R.; Romano, A. D.; Loguercio, C.; Serviddio, G.; Federico, A. Immunity as Cornerstone of Non-Alcoholic Fatty Liver Disease: The Contribution of Oxidative Stress in the Disease Progression. *Int. J. Mol. Sci.* **2021**, *22* (1), 436.
(16) Cataldi, M.; Manco, F.; Tarantino, G. Steatosis, Steatohepatitis and Cancer Immunotherapy: An Intricate Story. *Int. J. Mol. Sci.* **2021**, *22* (23), 12947.
(17) Granitzny, A.; Knebel, J.; Müller, M.; Braun, A.; Steinberg, P.; Dasenbrock, C.; Hansen, T. Evaluation of a human in vitro hepatocyte-NPC co-culture model for the prediction of idiosyncratic drug-induced liver injury: A pilot study. *Toxicology reports* **2017**, *4*, 89−103. From NLM Tasnim, F.; Huang, X.; Lee, C. Z. W.; Ginhoux, F.; Yu, H. Recent Advances in Models of Immune-Mediated Drug-Induced Liver Injury. *Frontiers in toxicology* **2021**, *3*, No. 605392. From NLM
(18) Müller, F. A.; Sturla, S. J. Human in vitro models of nonalcoholic fatty liver disease. *Current Opinion in Toxicology* **2019**, *16*, 9−16.
(19) Soret, P. A.; Magusto, J.; Housset, C.; Gautheron, J. In Vitro and In Vivo Models of Non-Alcoholic Fatty Liver Disease: A Critical Appraisal. *J. Clin. Med.* **2020**, *10* (1), 36.
(20) Cichoż-Lach, H.; Michalak, A. Oxidative stress as a crucial factor in liver diseases. *World journal of gastroenterology* **2014**, *20* (25), 8082−8091. From NLM
(21) Friedman, S. L.; Neuschwander-Tetri, B. A.; Rinella, M.; Sanyal, A. J. Mechanisms of NAFLD development and therapeutic strategies. *Nature medicine* **2018**, *24* (7), 908−922. From NLM
(22) Chen, Y.; Liu, Y.; Chen, S.; Zhang, L.; Rao, J.; Lu, X.; Ma, Y. Liver organoids: a promising three-dimensional model for insights

and innovations in tumor progression and precision medicine of liver cancer. *Front Immunol* **2023**, *14*, No. 1180184. From NLM
(23) Flores, Y. N.; Amoon, A. T.; Su, B.; Velazquez-Cruz, R.; Ramírez-Palacios, P.; Salmerón, J.; Rivera-Paredez, B.; Sinsheimer, J. S.; Lusis, A. J.; Huertas-Vazquez, A.; et al. Serum lipids are associated with nonalcoholic fatty liver disease: a pilot case-control study in Mexico. *Lipids in Health and Disease* **2021**, *20* (1), 136.
(24) Xiong, J.; Chen, X.; Zhao, Z.; Liao, Y.; Zhou, T.; Xiang, Q. A potential link between plasma short-chain fatty acids, TNF-α level and disease progression in non-alcoholic fatty liver disease: A retrospective study. *Experimental and therapeutic medicine* **2022**, *24* (3), 598. From NLM
(25) Coutinho, A. E.; Chapman, K. E. The anti-inflammatory and immunosuppressive effects of glucocorticoids, recent developments and mechanistic insights. *Molecular and cellular endocrinology* **2011**, *335* (1), 2−13. From NLM
(26) Tarantino, G.; Sinatti, G.; Citro, V.; Santini, S., Jr.; Balsano, C. Sarcopenia, a condition shared by various diseases: can we alleviate or delay the progression? *Internal and Emergency Medicine* **2023**, *18* (7), 1887−1895.
(27) Petrescu, M.; Vlaicu, S. I.; Ciumărnean, L.; Milaciu, M. V.; Mărginean, C.; Florea, M.; Vesa Ş, C.; Popa, M. Chronic Inflammation-A Link between Nonalcoholic Fatty Liver Disease (NAFLD) and Dysfunctional Adipose Tissue. *Medicina* **2022**, *58* (5), 641.
(28) Mirea, A. M.; Tack, C. J.; Chavakis, T.; Joosten, L. A. B.; Toonen, E. J. M. IL-1 Family Cytokine Pathways Underlying NAFLD: Towards New Treatment Strategies. *Trends in molecular medicine* **2018**, *24* (5), 458−471. From NLM
(29) Wieckowska, A.; Papouchado, B. G.; Li, Z.; Lopez, R.; Zein, N. N.; Feldstein, A. E. Increased hepatic and circulating interleukin-6 levels in human nonalcoholic steatohepatitis. *American journal of gastroenterology* **2008**, *103* (6), 1372−1379. From NLM
(30) Kirovski, G.; Dorn, C.; Huber, H.; Moleda, L.; Niessen, C.; Wobser, H.; Schacherer, D.; Buechler, C.; Wiest, R.; Hellerbrand, C. Elevated systemic monocyte chemoattractrant protein-1 in hepatic steatosis without significant hepatic inflammation. *Experimental and molecular pathology* **2011**, *91* (3), 780−783. From NLM Tilg, H. The role of cytokines in non-alcoholic fatty liver disease. *Digestive diseases (Basel, Switzerland)* **2010**, *28* (1), 179−185. From NLM
(31) Abdal Dayem, A.; Hossain, M. K.; Lee, S. B.; Kim, K.; Saha, S. K.; Yang, G.-M.; Choi, H. Y.; Cho, S.-G. The Role of Reactive Oxygen Species (ROS) in the Biological Activities of Metallic Nanoparticles. *Int. J. Mol. Sci.* **2017**, *18* (1), 120.
(32) Peng, C.; Stewart, A. G.; Woodman, O. L.; Ritchie, R. H.; Qin, C. X. Non-Alcoholic Steatohepatitis: A Review of Its Mechanism, Models and Medical Treatments. *Frontiers in pharmacology* **2020**, *11*, No. 603926. From NLM.
(33) Tarantino, G.; Citro, V. What are the common downstream molecular events between alcoholic and nonalcoholic fatty liver? *Lipids in Health and Disease* **2024**, *23* (1), 41.
(34) Blache, U.; Weiss, R.; Boldt, A.; Kapinsky, M.; Blaudszun, A.-R.; Quaiser, A.; Pohl, A.; Miloud, T.; Burgaud, M.; Vucinic, V.; et al. Advanced Flow Cytometry Assays for Immune Monitoring of CAR-T Cell Applications. *Front. Immunol.* **2021**, *12*, No. 658314, DOI: 10.3389/fimmu.2021.658314.
(35) Pinyopornpanish, K.; Leerapun, A.; Pinyopornpanish, K.; Chattipakorn, N. Effects of Metformin on Hepatic Steatosis in Adults with Nonalcoholic Fatty Liver Disease and Diabetes: Insights from the Cellular to Patient Levels. *Gut and liver* **2021**, *15* (6), 827−840. From NLM Ramms, B.; Patel, S.; Sun, X.; Pessentheiner, A. R.; Ducasa, G. M.; Mullick, A. E.; Lee, R. G.; Crooke, R. M.; Tsimikas, S.; Witztum, J. L.; et al.Interventional hepatic apoC-III knockdown improves atherosclerotic plaque stability and remodeling by triglyceride lowering. *JCI insight***2022**, *7* (13). DOI: DOI: 10.1172/jci.insight.158414 From NLM.

https://doi.org/10.1021/acsomega.4c02433
ACS Omega 2024, 9, 25094−25105